

# Quantum Parameter Space of Dissipative Directed Transport

Leonardo Ermann and Gabriel G. Carlo

*Departamento de Física, CNEA, Libertador 8250, (C1429BNP) Buenos Aires, Argentina\**

(Dated: October 14, 2014)

Quantum manifestations of isoperiodic stable structures (QISSs) have a crucial role in the current behavior of quantum dissipative ratchets. In this context, the simple shape of the ISSs has been conjectured to be an almost exclusive feature of the classical system. This has drastic consequences for many properties of the directed currents, the most important one being that it imposes a significant reduction in their maximum values, thus affecting the attainable efficiency at the quantum level. In this work we prove this conjecture by means of comprehensive numerical explorations and statistical analysis of the quantum states. We are able to describe the *quantum parameter space* of a paradigmatic system for different values of  $\hbar_{\text{eff}}$  in great detail. Moreover, thanks to this we provide evidence on a mechanism that we call *parametric tunneling* by which the sharp classical borders of the regions in parameter space become blurred in the quantum counterpart. We expect this to be a common property of generic dissipative quantum systems.

PACS numbers: 05.60.Gg, 05.45.Mt

The idea of directed transport [1] proved to be very fruitful, and has attracted a huge interest in recent years [2]. It can be very briefly defined as transport phenomena in spatial and time periodic systems which are not subject to thermal equilibrium. The current appears since all spatiotemporal symmetries leading to momentum inversion are broken [3]. Examples of ratchet models (as they are also usually referred to) have found application in many areas of research. Here we will mention just a few, such as biology [4], nanotechnology [5], granular crystals [6], and some chemical reactions as isomerization [7]. This gives an idea of how different the fields of interest could be.

At the classical level, deterministic ratchets with dissipation are generally associated with an asymmetric chaotic attractor [8]. Quantum ratchets show very rich behavior [9]. In this respect we should mention that cold atoms in optical lattices have been deeply investigated from both, the theoretical and experimental points of view [10, 11]. This extends also to Bose-Einstein condensates, which have been transported by means of quantum ratchet accelerators [12], where the current has no classical counterpart [13] and the energy grows ballistically [14, 15]. Within this framework, a dissipative quantum ratchet interesting for cold atoms experiments has been introduced in [16]. Very recently, the parameter space of the classical counterpart of this system has been the object of a detailed study [17, 18]. There it has been found that families of isoperiodic stable structures (ISSs are Lyapunov stable islands, generic in the parameter space of dissipative systems), have a very important role in the description of the currents. Subsequently, the effects of temperature have been included in the investigations leading to the determination of resistant optimal ratchet transport in its presence [19].

When looking at the quantum counterparts of these

structures it has recently been found that in general the QISSs look like the quantum chaotic attractors at their vicinity in parameter space [20]. In other words, the simple structure of the classical ISSs has been conjectured to be an almost exclusive property of the classical system. Just in comparatively few cases the quantum structures are similar to these classically simple objects (periodic points in the case of maps). One of the main results of this paper consists of providing with a comprehensive proof to this conjecture. For that purpose, we give a complete description of the *quantum parameter space* for two different  $\hbar_{\text{eff}}$  values. On the other hand, we show how the regions that can be associated to ISSs families become interwoven at the quantum level, blurring their classically sharp borders, and thus giving rise to what we call *parametric tunneling*.

The system under investigation is a paradigmatic dissipative ratchet system given by the map [16, 19, 20]

$$\begin{cases} \bar{n} = \gamma n + k[\sin(x) + a \sin(2x + \phi)], \\ \bar{x} = x + \tau \bar{n}, \end{cases} \quad (1)$$

where we have denoted by  $n$  the momentum variable conjugated to  $x$ ,  $\tau$  being the period of the map and  $\gamma$  the dissipation parameter. These equations describe a particle moving in one dimension [ $x \in (-\infty, +\infty)$ ] subjected to the periodic kicked asymmetric potential

$$V(x, t) = k \left[ \cos(x) + \frac{a}{2} \cos(2x + \phi) \right] \sum_{m=-\infty}^{+\infty} \delta(t - m\tau), \quad (2)$$

again  $\tau$  is the kicking period, having a dissipation parametrized by  $0 \leq \gamma \leq 1$ .  $\gamma = 0$  corresponds to the particle in the overdamped regime and  $\gamma = 1$  to the conservative evolution. The directed transport appears due to broken spatial ( $a \neq 0$  and  $\phi \neq m\pi$ ) and temporal ( $\gamma \neq 1$ ) symmetries, we take  $a = 0.5$  and  $\phi = \pi/2$  in this work. The classical dynamics depends only on the parameter  $K = k\tau$ , which can be directly noticed when introducing the rescaled momentum  $p = \tau n$ .

\* ermann@tandar.cnea.gov.ar, carlo@tandar.cnea.gov.ar

The quantum version can be obtained following a standard procedure:  $x \rightarrow \hat{x}$ ,  $n \rightarrow \hat{n} = -i(d/dx)$  ( $\hbar = 1$ ). Since  $[\hat{x}, \hat{p}] = i\tau$ , the effective Planck constant is  $\hbar_{\text{eff}} = \tau$ . The classical limit corresponds to  $\hbar_{\text{eff}} \rightarrow 0$ , while  $K = \hbar_{\text{eff}}k$  remains constant. Dissipation can be introduced thanks to the master equation [21] for the density operator  $\hat{\rho}$  of the system

$$\dot{\hat{\rho}} = -i[\hat{H}_s, \hat{\rho}] - \frac{1}{2} \sum_{\mu=1}^2 \{\hat{L}_\mu^\dagger \hat{L}_\mu, \hat{\rho}\} + \sum_{\mu=1}^2 \hat{L}_\mu \hat{\rho} \hat{L}_\mu^\dagger. \quad (3)$$

Here  $\hat{H}_s = \hat{n}^2/2 + V(\hat{x}, t)$  is the system Hamiltonian,  $\{, \}$  is the anticommutator, and  $\hat{L}_\mu$  are the Lindblad operators given by

$$\begin{aligned} \hat{L}_1 &= g \sum_n \sqrt{n+1} |n\rangle \langle n+1|, \\ \hat{L}_2 &= g \sum_n \sqrt{n+1} |-n\rangle \langle -n-1|, \end{aligned} \quad (4)$$

with  $n = 0, 1, \dots$  and  $g = \sqrt{-\ln \gamma}$  (according to the Ehrenfest theorem). We have evolved  $10^6$  classical random initial conditions having  $p \in [-\pi, \pi]$  and  $x \in [0, 2\pi]$  ( $\langle p_0 \rangle = 0$ ) in all cases, and also their quantum density operator counterpart in a Hilbert space of dimension  $N$ .

In [17–19] several classical parameter space portraits have been shown. Thanks to them three main kinds of ISSs were identified and called  $B_M$ ,  $C_M$  and  $D_M$ , where  $M$  stands for an integer or rational number and corresponds to the mean momentum of these structures in units of  $2\pi$ . With the exception of  $\gamma \rightarrow 1$  (i.e., near the conservative limit), ISSs organize the parameter space structure and then are essential to understand the current behavior. In previous work [20], sampling a set of relevant points in the quantum parameter space has been the only possibility, due to computational restrictions. In this paper we report a major breakthrough in this direction, since we were able to completely extend these classical results and provide with quantum parameter space portraits in the areas of interest. This can be seen in Fig 1, where we show the quantum current  $J_q$  (we take  $J_q, J_c = \langle p \rangle$ , where  $\langle p \rangle$  stands for either the quantum or classical average momentum, respectively) as a function of parameters  $k$  and  $\gamma$ . The upper panel corresponds to  $\hbar_{\text{eff}} = 0.411$ , while the lower one to  $\hbar_{\text{eff}} = 0.137$ , both having a resolution of  $170 \times 100$  points. They have been obtained by using a cluster having more than 100 processors. It is noticeable how the large  $B_1$  structure is almost the only clearly recognizable feature that resembles the classical ISSs found in parameter space. There is also a poorly defined region of positive current that can be attributed to one of the higher order  $B$  families. However, the areas associated to chaotic attractors are recognizable, specially the one at  $k \sim [3.0, 4.0]$  and  $\gamma \sim [0.6, 0.8]$ .

In order to investigate what happens with the other ISSs that seem not to have a quantum counterpart and also the behavior of the  $B_1$  QISS, we explore the three highlighted regions ((green) gray squares) of Fig. 1 in more detail. In Fig. 2 we show zooms ( $100 \times 100$  points)

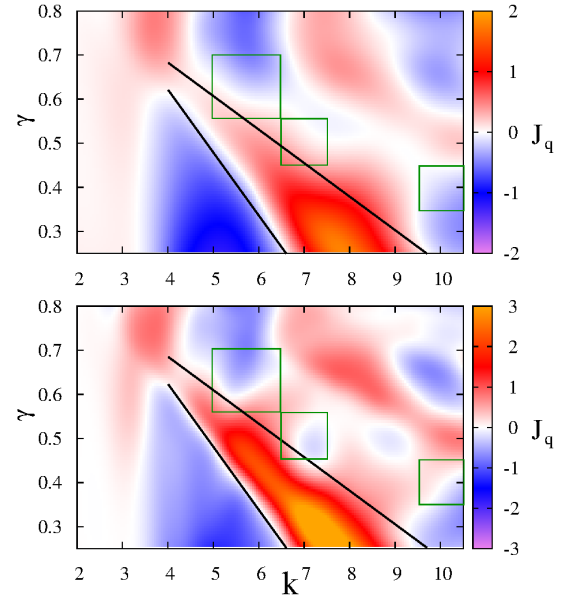


FIG. 1. (color online) Quantum current  $J_q$  as a function of parameters  $k$  and  $\gamma$  in a grid of  $170 \times 100$  points. The upper panel corresponds to  $\hbar_{\text{eff}} = 0.411$ , while the lower one to  $\hbar_{\text{eff}} = 0.137$ . Black lines correspond to the classical sharp borders of the  $B_1$  structure (as in Fig. 1 of [17]). (Green) gray squares highlight the regions shown in Fig. 2.

taken inside these areas, the upper row corresponding to  $\hbar_{\text{eff}} = 0.411$  and the lower one to  $\hbar_{\text{eff}} = 0.137$ . In the left column we can appreciate how the largest of the  $C$  structures ( $C_{-1}$ ) influences the  $B_1$  region. This causes a lowering of the current inside the positive ISS region that is remarkably more pronounced in the  $\hbar_{\text{eff}} = 0.137$  case than for  $\hbar_{\text{eff}} = 0.411$ . This indicates a kind of tunneling of one structure into the other and since this takes place in the parameter space, we propose it as the definition of parametric tunneling. Also, there is a positive current chaotic region different from the  $B_1$  structure but contiguous to it, that forms a continuum with  $B_1$  at the quantum level. The middle column shows the next zoom area that is connected with the previous one by its upper-left corner as can be seen in Fig 1 panels. It shares the mentioned positive current region and also has a negative current chaotic zone. This latter also has an influence on the  $B_1$  structure, phenomenon that is clearly more marked for the lower  $\hbar_{\text{eff}} = 0.137$  case and that can be appreciated with the help of the Fig. 2 middle lower panel. Finally, the right column shows an isolated area corresponding to one part of the  $D_{-1}$  structure which seems to faintly manifest itself through negative currents but whose shape makes it difficult to precisely relate it to its classical counterpart. In fact it seems to be merged with the negative current chaotic region embedding it.

In order to systematically prove that simple (point-like) structures are exceptional at the quantum level, we have analyzed the shape of the limiting quantum momentum distributions (obtained after 50 time steps) by

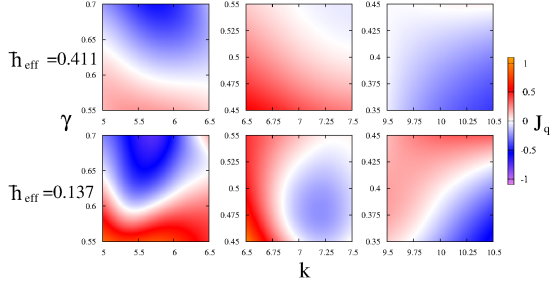


FIG. 2. (color online) Quantum current  $J_q$  for the three different regions highlighted by means of (green) gray squares in Fig. 1. The upper panels correspond to  $\hbar_{\text{eff}} = 0.411$ , while the lower ones to  $\hbar_{\text{eff}} = 0.137$ , all grids are of  $100 \times 100$  points.

means of the participation ratio  $\eta = (\sum_i P(p_i)^2)^{-1}/N$ . This measure is a good indicator of the fraction of basis elements that effectively expands the quantum state. For comparative purposes we have also calculated the corresponding classical  $\eta$  by taking a discretized  $p$  distribution (after 10000 time steps), having a number of bins given by the Hilbert space dimension of the lower  $\hbar_{\text{eff}}$  case (this being  $N = 3^6$ ). It is clear that a finer coarse-graining would slightly change the classical  $\eta$  distributions but this will not affect their main properties. This is because the distance among points of the ISSs is almost always greater than the chosen bin size. We have calculated the histograms  $P_\eta$  vs.  $\eta$ , and we have also studied how  $\eta$  behaves as a function of the current  $J_q, J_c$ . Results are shown in Fig. 3, where the upper panel corresponds to the histograms (normalized to 1) for all the cases shown in Fig. 1. The classical  $P_\eta$  values (black circles and solid line) have a peak at extremely low  $\eta$ , which can be seen in the inset. The quantum  $P_\eta$  for  $\hbar_{\text{eff}} = 0.411$  ((red) dark gray squares and dotted line) and  $\hbar_{\text{eff}} = 0.137$  ((green) light gray diamonds and dashed line) have larger values at the tail of the distributions. These are the most important properties and they are enough to prove our conjecture. Moreover, with the exception of the peak around  $\eta = 0.2$  the classical distribution falls below 0.01 very quickly, while the quantum ones acquire finite values after  $\eta \sim 0.03$ . On the other hand the quantum distribution for  $\hbar_{\text{eff}} = 0.137$  starts to follow the shape of the classical one for higher  $\eta$  but it is almost unchanged with respect to  $\hbar_{\text{eff}} = 0.411$  for the lowest values. In Fig. 3 bottom left panel we can see that the maximum  $J_c$  correspond to the lowest  $\eta$ , and when superimposed to the quantum values (see Fig. 3 bottom right panel) they roughly match them for some of the lowest  $J_q, J_c$ . In general the classical  $\eta$  are extremely discontinuous, a signature of the classical sharp borders of the different regions in parameter space, while the quantum ones behave smoothly, also reflecting the appearance of the corresponding quantum parameter space. It is worth mentioning that the maximum of  $J_q$  is attained for one of the lowest  $\eta$  values and that can be associated to the “core” of the  $B_1$  region (around  $k = 7.5$

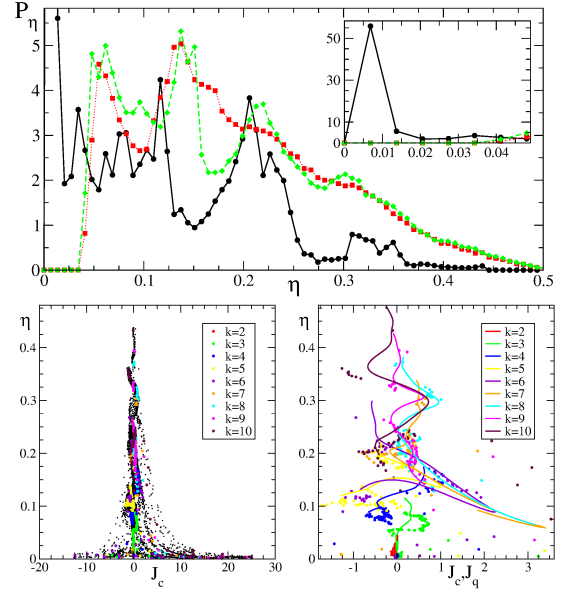


FIG. 3. (color online) Top panel shows the participation ratio histograms  $P_\eta$  as a function of  $\eta$ . Statistics corresponds to all the cases shown in Fig. 1. Classical  $P_\eta$  is represented with black circles (solid line), and quantum  $P_\eta$  for  $\hbar_{\text{eff}} = 0.411$  and  $\hbar_{\text{eff}} = 0.137$  with (red) dark gray squares (dotted line) and (green) light gray diamonds (dashed line), respectively. Inset shows the same histograms in the  $\eta \in [0 : 0.05]$  range. Bottom left panel: black circles represent  $\eta$  as a function of  $J_c$ , with integer values of  $k$  in different (colors) grays. Bottom right panel: comparison of classical (circles) and quantum (lines)  $\eta$  as a function of  $J_q, J_c$  for  $\hbar_{\text{eff}} = 0.137$  with integer values of  $k = 2, \dots, 10$  and 100 values of  $\gamma \in [0.2, 0.8]$ .

and  $\gamma = 0.3$ ). The few lower quantum  $\eta$  values have also much lower  $J_q$  and belong to the lowest  $k$  region.

Finally, we have selected transversal cuts of Fig. 1 for two different  $\gamma$  values, these being 0.45, and 0.55. This shows that the classical features are very slowly approached by the quantum distributions and also how different parameter space neighboring regions influence each other. The results are shown in Fig. 4 upper and bottom panels respectively, where it is important to notice that the classical current scale (on the right side) is much larger than the quantum one (on the left side). It is clearly visible that the sharp borders corresponding to the classical regions cannot be reproduced by the quantum counterparts, even though the current significantly grows as  $\hbar_{\text{eff}}$  drops from 0.411 to 0.068 for the  $B$  QISSs. Moreover we see how negative  $J_q, J_c$  values, typical of the chaotic region near  $B_1$  that is highlighted in the middle panels of Fig. 2, also can be found inside a small portion of the  $B_1$  area near its border (see Fig. 4 upper panel). The influence suffered from the  $C_{-1}$  structure near  $B_1$  can be appreciated as a clear drop in  $J_q$  values inside the region corresponding to this structure (see Fig. 4 bottom panel). Again, it is remarkable that this phenomenon is more pronounced for the lowest  $\hbar_{\text{eff}} = 0.068$  value.

To summarize, we have performed a comprehensive ex-

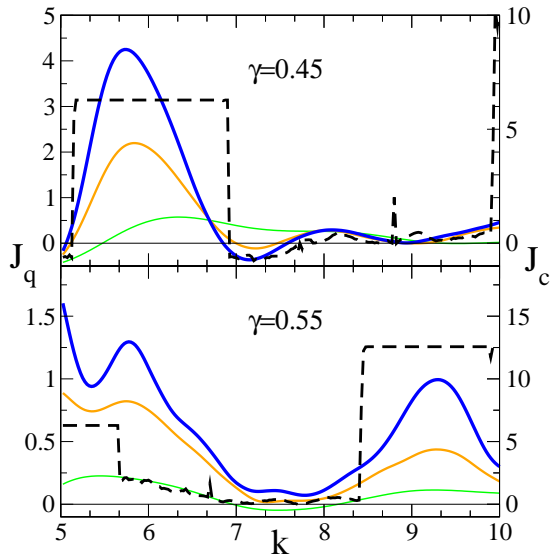


FIG. 4. (color online) Quantum and classical current  $J_q$  and  $J_c$  as a function of parameter  $k$  for  $\gamma = 0.45$  (top panel), and  $\gamma = 0.55$  (bottom panel). Quantum currents are represented with solid (green) light gray lines for  $\hbar_{\text{eff}} = 0.411$ , (orange) gray lines for  $\hbar_{\text{eff}} = 0.137$ , and (blue) dark gray lines for  $\hbar_{\text{eff}} = 0.068$ . Their corresponding scales are shown on the left side. Classical currents are illustrated with dashed black lines with their corresponding scales on the right.

ploration of the quantum parameter space of a paradigmatic system in the directed transport, open systems and quantum chaos literature, i.e. the dissipative quantum kicked rotator with a biharmonic kick. As a result we were able to develop a complete picture of the *quantum parameter space* for this kind of systems. Thanks to statistically exploring the limiting distributions through the participation ratios  $\eta$ , we have systematically proved that the simple structure of the classical ISSs is exceptional at the quantum level. This is of huge relevance for the properties of quantum directed currents, mainly limiting their maximum values and as such, reducing the efficiency. Moreover, we have found a remarkable feature of QISSs, this being the influence that they suffer among each other that blurs their classically sharp borders, a phenomenon we have called *parametric tunneling*. In the future, we will try to identify the details behind this mechanism and also its consequences at the current level. Also, we plan to consider a non zero temperature in order to test how robust is the obtained quantum parameter space picture.

Financial support from CONICET is gratefully acknowledged.

- 
- [1] R. P. Feynman, *Lectures on Physics*, **Vol. 1**, (Addison-Wesley, Reading, MA, 1963).
  - [2] P. Reimann, Phys. Rep. **361**, 57 (2002); S. Kohler, J. Lehmann, and P. Hänggi, Phys. Rep. **406**, 379 (2005); S. Denisov, S. Flach, and P. Hänggi, Phys. Rep. **538**, 77 (2014).
  - [3] S. Flach, O. Yevtushenko, and Y. Zolotaryuk, Phys. Rev. Lett. **84**, 2358 (2000).
  - [4] G. Mahmud *et al.*, Nature Phys. **5**, 606 (2009); G. Lambert, D. Liao, and R.H. Austin, Phys. Rev. Lett. **104**, 168102 (2010); S. Cocco, J.F. Marko, and R. Monasson, Phys. Rev. Lett. **112**, 238101 (2014).
  - [5] R. D. Astumian, Science **276**, 917 (1997); D. Reguera, A. Luque, P.S. Burada, G. Schmid, J.M. Rubí, and P. Hänggi, Phys. Rev. Lett. **108**, 020604 (2012).
  - [6] V. Berardi, J. Lydon, P.G. Kevrekidis, C. Daraio, and R. Carretero-González, Phys. Rev. E **88**, 052202 (2013).
  - [7] G. G. Carlo, L. Ermann, F. Borondo, and R. M. Benito, Phys. Rev. E **83**, 011103 (2011); L.S. Brizhik, A.A. Eremko, B.M.A.G. Piette, and W.J. Zakrzewski, Phys. Rev. E **89**, 062905 (2014).
  - [8] J. L. Mateos, Phys. Rev. Lett. **84**, 258 (2000).
  - [9] P. Reimann, M. Grifoni, and P. Hänggi, Phys. Rev. Lett. **79**, 10 (1997); L. Ermann, G. G. Carlo, and M. Saraceno, Phys. Rev. E **77**, 011126 (2008); L. Ermann, G. G. Carlo, and M. Saraceno, Phys. Rev. E **79**, 056201 (2009).
  - [10] T. Salger, S. Kling, T. Hecking, C. Geckeler, L. Morales-Molina, and M. Weitz, Science **326**, 1241 (2009).
  - [11] T. S. Monteiro, P. A. Dando, N. A. C. Hutchings, and M. R. Isherwood, Phys. Rev. Lett. **89**, 194102 (2002); G. G. Carlo, G. Benenti, G. Casati, S. Wimberger, O. Morsch, R. Mannella, and E. Arimondo, Phys. Rev. A **74**, 033617 (2006).
  - [12] M. Sadgrove, M. Horikoshi, T. Sekimura, and K. Nakagawa, Phys. Rev. Lett. **99**, 043002 (2007); I. Dana, V. Ramareddy, I. Talukdar, and G.S. Summy, Phys. Rev. Lett. **100**, 024103 (2008); D.H. White, S.K. Ruddell, and M.D. Hoogerland Phys. Rev. A **88**, 063603 (2013).
  - [13] E. Lundh and M. Wallin, Phys. Rev. Lett. **94**, 110603 (2005); D. Poletti, G. G. Carlo, and B. Li, Phys. Rev. E **75**, 011102 (2007).
  - [14] A. Kenfack, J. Gong, and A.K. Pattanayak, Phys. Rev. Lett. **100**, 044104 (2008); J. Wang and J. Gong, Phys. Rev. E **78**, 036219 (2008).
  - [15] M. Sadgrove, M. Horikoshi, T. Sekimura, and K. Nakagawa, Eur. Phys. J. D **45**, 229 (2007).
  - [16] G. G. Carlo, G. Benenti, G. Casati, and D.L. Shepelyansky, Phys. Rev. Lett. **94**, 164101 (2005).
  - [17] A. Celestino, C. Manchein, H.A. Albuquerque, and M.W. Beims, Phys. Rev. Lett. **106**, 234101 (2011).
  - [18] A. Celestino, C. Manchein, H.A. Albuquerque, and M.W. Beims, Commun. Nonlinear Sci. Numer. Simulat. **19**, 139 (2014).
  - [19] C. Manchein, A. Celestino, and M.W. Beims, Phys. Rev. Lett. **110**, 114102 (2013).
  - [20] G. G. Carlo, Phys. Rev. Lett. **108**, 210605 (2012).
  - [21] G. Lindblad, Commun. Math. Phys. **48**, 119 (1976).